

1 Debris-flow volume quantile prediction
2 from catchment morphometry

3 **Tjalling de Haas^{1,2} and Alexander L. Densmore¹**

4 *¹Institute of Hazard, Risk, and Resilience, Department of Geography, Durham University,*
5 *Durham DH1 3LE, UK*

6 *²Department of Physical Geography, Universiteit Utrecht, Princetonlaan 8a, 3584 CB Utrecht,*
7 *The Netherlands*

8

9 **ABSTRACT**

10 Estimation of the volumes of potential future debris flows is key for hazard assessment
11 and mitigation. Worldwide, however, there are few catchments for which detailed volume-
12 frequency information is available. We (1) reconstruct volume-frequency curves for 10 debris-
13 flow catchments in Saline Valley, California, USA, from a large number of well-preserved,
14 unmodified surficial flow deposits, and (2) assess the correlations between lobe-volume quantiles
15 and a set of morphometric catchment characteristics. We find statistically significant correlations
16 between lobe-volume quantiles, including median and maximum, and catchment relief, length
17 (planimetric distance from the fan apex to the most distant point along the watershed boundary),
18 perimeter, and Melton ratio (relief divided by the square root of catchment area). These findings
19 show that it may be possible to roughly estimate debris-flow lobe-volume quantiles from basic
20 catchment characteristics that can be obtained from globally available elevation data. This may
21 assist design-volume estimation in debris-flow catchments where past flow volumes are
22 otherwise unknown.

23

24 INTRODUCTION

25 Debris flows are dense masses of sediment and water that are common in mountainous
26 terrain, and that create low-gradient ($<15^\circ$) sediment fans through repeated deposition over time.
27 Such debris-flow fans are preferred locations for development in many mountainous regions
28 (Jakob, 2005). Estimation of both past and potential future flow volumes on fan surfaces is
29 critical for assessment of flow hazard and design of mitigation measures, because flow volume is
30 a prime control on flow velocity, peak discharge, and inundation area (e.g., Iverson et al., 1998;
31 Rickenmann, 1999; Griswold and Iverson, 2008). A global analysis of debris-flow hazards
32 between 1950 and 2011 shows that the number of fatalities increases exponentially with flow
33 volume (Dowling and Santi, 2014). Ideally, we should know the full flow volume-frequency
34 distribution, because maximum volumes are relevant for hazard assessment while median
35 volumes are relevant for sediment budget estimation (Bovis and Jakob, 1999).

36 Worldwide, however, there are very few catchments for which detailed volume-
37 frequency information is available (e.g., Jakob and Friele, 2010; Bennett et al., 2014). The
38 debris-flow volume reaching a fan depends on the amount of sediment available and the potential
39 of the flow to mobilize and transport this sediment, and is thus a function of catchment
40 morphometry, morphology, and geology as well as hydroclimatic conditions (e.g., Hungr et al.,
41 1984; Bovis and Jakob, 1999). In most systems, debris rather than water availability is the
42 dominant control on flow volume (e.g., Jakob and Bovis, 1996; Bovis and Jakob, 1999). Many
43 researchers have therefore attempted to correlate debris-flow volume with morphometric
44 catchment characteristics, predominantly catchment area and slope and channel length (e.g.,
45 Hungr et al., 1984; Jakob and Bovis, 1996; Marchi and D'Agostino, 2004; Ma et al., 2013). A

46 major shortcoming of these correlations is that they are based on only one to a few debris flows
47 per catchment, inhibiting estimation of key flow-volume quantiles such as the median and
48 maximum. It has been difficult to overcome this issue because of both the brevity of
49 observational records relative to typical debris-flow return periods and the difficulty of
50 determining flow volume directly, even in well-instrumented catchments with frequent flows
51 (Schürch et al., 2011).

52 Fan surfaces are a potential archive of volume information for a large number of flows
53 (e.g., Jakob et al., 2016). Debris flows deposit sediment levees and lobes (e.g., Blair and
54 McPherson, 2009) whose dimensions may scale with the volume or peak discharge of the flow
55 (Berti and Simoni, 2007). Unfortunately, debris-flow deposits are often reworked by post-
56 depositional sediment transport processes or buried by subsequent flows, both of which obscure
57 the original deposit dimensions and hinder volume estimation (e.g., Jakob and Bovis, 1996; Blair
58 & McPherson, 2009; De Haas et al., 2014). In addition, large debris flows tend to spread out to
59 form multiple lobe deposits, making it difficult to reconstruct the entire flow volume – especially
60 if parts of the deposit are later reworked. As a result, the links between fan deposits, flow-
61 volume quantiles, and the potential controls on flow volumes have not yet been comprehensively
62 explored.

63 Here, we use the surfaces of 10 remarkably well-preserved debris-flow fans in Saline
64 Valley, southwestern USA, which host numerous unmodified flow deposits, to: (1) create lobe
65 volume-frequency curves from hundreds of well-preserved surficial debris-flow deposits; and (2)
66 use these to assess the correlation between lobe-volume quantiles and a set of morphometric
67 catchment characteristics, in order to explore and develop a method for debris-flow design
68 volume estimation.

69

70 **STUDY AREA**

71 Saline Valley is a closed extensional basin located at the boundary between the Mojave
72 and Great Basin deserts in southeastern California, USA (Fig. 1). The southern and western
73 valley margins host a series of well-exposed debris-flow fans that have developed in response to
74 accommodation generation by slip on the Hunter Mountain and Saline Valley faults (Oswald and
75 Wesnousky, 2002). We focus on 10 of those fans whose surfaces preserve abundant debris-flow
76 deposits with clear primary flow features and negligible secondary modification.

77 Eight fans, S01-08, originate from the Nelson Range in the southern part of the valley
78 (Fig. 1). The Nelson Range is underlain by the Early Jurassic Hunter Mountain quartz monzonite
79 batholith (Oswald and Wesnousky, 2002). Fan S03 is fed by two subcatchments, each of which
80 contributes sediment to a separate part of the fan surface. We treat those two subcatchments and
81 their corresponding fan surfaces as individual systems in the analyses presented here.

82 A ninth debris-flow fan, N01, originates from the Inyo Mountains in the northern part of
83 Saline Valley (Fig. 1). The catchment of this fan consists mostly of Paleozoic marble, quartzite,
84 and chert with a small area of quartz monzonite in the catchment headwaters (Conrad and
85 McKee, 1985).

86 Saline Valley is located in the rain shadow of the Sierra Nevada and Inyo Mountain
87 ranges to the west, with mean annual precipitation of 100-200 mm (PRISM, 2015). Historical
88 records in nearby Owens Valley show that recent debris flows in the region have been
89 predominantly triggered by high-intensity summer rainstorms (e.g., Beaty, 1963; Blair and
90 McPherson, 1998).

91

92 **DATA COLLECTION AND ANALYSIS**

93 We estimated debris-flow lobe volumes from a gridded LiDAR dataset with 0.5 m
94 horizontal cell size (Suppl. Fig. 1), collected in April 2007 by the National Center for Airborne
95 Laser Mapping (NCALM). Debris-flow lobe deposits were manually identified and mapped
96 using hillshade, curvature, and local slope maps (cf. Staley et al., 2006; Roering et al., 2013),
97 cross-checked by field measurements in September 2017 (Suppl. Fig. 2). Lobe thickness h [m]
98 was measured by defining the maximum thickness of a lobe extracted from elevation cross- and
99 long-profiles, assuming a planar bed underneath the lobe deposits (Suppl. Fig. 1). Lobe width w
100 [m] was defined as the maximum width of the lobe deposit. The cross-sectional area of each
101 debris-flow lobe A_l [m²] was then calculated by assuming a trapezoidal cross-section (cf. De
102 Haas et al., 2015):

103
$$A_l = 0.75 h w \quad \text{Eq. 1}$$

104 We assumed a conservative uncertainty on A_l of 50%, accounting for variation between
105 triangular and rectangular cross-sections and deviations from a planar bed. Iverson et al. (1999)
106 and Griswold and Iverson (2008) showed that the cross-sectional area of a debris flow is a semi-
107 empirical function of its total volume V [m³]:

108
$$A_l = \varepsilon V^{2/3} \quad \text{Eq. 2}$$

109 Based on 15 recent non-buried debris flows we find $\varepsilon \approx 0.1$ for the Saline Valley fans (R^2
110 = 0.82; Suppl. Fig. 3), similar to the ε found by Griswold and Iverson (2008) for 50 non-volcanic
111 debris flows worldwide. The estimated debris-flow volumes are accurate within a factor 2
112 (Suppl. Fig. 3). For our calculation we assume $\varepsilon = 0.1 \pm 0.025$. We used eq. 2 to convert the
113 measured cross-sectional areas to total lobe volumes, propagating the errors in A_l and ε .

114 Direct measurement of total flow volumes is generally not possible for all but the most
115 recent flows due to burial by more recent deposits. For the same reason, we typically cannot
116 identify whether individual flows deposited one or multiple lobes. Note that the volume of the
117 largest debris flows, which are most likely to have formed multiple lobes, may thus have been
118 underestimated (e.g., Blair and McPherson, 1998; De Haas et al., 2016; 2018).

119 We compared the inferred debris-flow lobe volumes to a wide range of morphometric
120 catchment characteristics (Table 1). The LiDAR dataset does not cover the full fan catchments,
121 and therefore we used ASTER Global Digital Elevation Model (GDEM) data to infer these
122 catchment characteristics. This elevation data set is globally available and has a 30 m horizontal
123 resolution, ensuring worldwide applicability but limiting our analysis to simple catchment
124 characteristics. We assessed the correlations between catchment characteristics and the 25, 50,
125 75, and 99 percentiles and maximum lobe-volume quantiles through linear regression.

126

127 **RESULTS**

128 The number of individual debris-flow lobe deposits identified on the fans ranges from 84
129 on fan S03b to 851 on fan S06 (Fig. 2). The smallest reconstructed median debris-flow lobe
130 volume, $140 \pm 55 \text{ m}^3$, was found on fan S03b. The largest median lobe volume, $830 \pm 330 \text{ m}^3$,
131 was found on fan S04. The reconstructed maximum lobe volumes range from $4400 \pm 1750 \text{ m}^3$ on
132 fan S02 to $92000 \pm 37000 \text{ m}^3$ on fan S07. The volume distribution curves highlight that the lobe
133 volumes on a single fan can vary by four orders of magnitude.

134 Overall, median lobe volume is the quantile that shows the best correlation with
135 catchment characteristics (Fig. 3). There are statistically significant correlations ($p < 0.05$)
136 between median lobe volume and catchment area, relief, length, perimeter, and Melton ratio

137 (Suppl. Tab. 1). The goodness-of-fit (R^2) of these correlations ranges between 0.39 and 0.51,
138 where Melton ratio performs best. There are also statistically significant relations between
139 maximum lobe volume and catchment relief, length, and perimeter, while the relation with
140 Melton ratio is close to significant with a p-value of 0.07. Catchment perimeter, length, relief and
141 Melton ratio generally show statistically significant correlations with most other lobe-volume
142 quantiles, and where correlations are statistically insignificant the p-values are nonetheless still
143 typically smaller than 0.1.

144 We find no statistically significant correlations and poor goodness-of-fit values, generally
145 below 0.20, between lobe-volume quantiles and mean catchment slope, relief ratio, form factor,
146 elongation ratio, and circularity index (Suppl. Tab. 1).

147 Our dataset shows two outliers in the relationships between lobe volume and catchment
148 area, relief, Melton ratio, perimeter and length, corresponding to the two smallest watersheds,
149 S02 and S03b (Fig. 3). These outliers have relatively small lobes, which for maximum volume
150 are almost one order of magnitude lower than would be expected based on the correlations with
151 catchment characteristics.

152 Based on our very limited sampling, differences in catchment lithology do not seem to
153 affect the lobe volume-catchment characteristic relationships in our dataset. The flow volumes
154 on fan N01, with a catchment that consists predominantly of metasedimentary rock, follow
155 similar relationships with catchment characteristics as those fed from the quartz monzonite
156 catchments (Fig. 3).

157

158 **DISCUSSION**

159 Our results show that, at least in climatically- and tectonically-similar areas, it may be
160 possible to predict debris-flow lobe-volume quantiles, including median and maximum, based on
161 catchment relief, perimeter, length, area and Melton ratio. These findings may assist in debris-
162 flow hazard assessment and mitigation where data on lobe or flow volumes are otherwise
163 unknown, which holds true for the vast majority of catchments. Moreover, our findings may help
164 to estimate sediment budgets where such data are otherwise unavailable (Bovis and Jakob,
165 1999). Although our data do not show how climatic and lithological conditions may affect lobe-
166 volume quantiles, we suggest that, where the flow-volume distribution of a debris-flow system is
167 known, flow volume quantiles in neighboring catchments may be reasonably estimated based on
168 a catchment relief, perimeter, length, area or Melton-ratio correction.

169 A number of studies have used catchment characteristics to discriminate between the likely
170 predominance of debris-flow and streamflow sediment transport. In particular, catchment area
171 (e.g., de Scally and Owens, 2004), length (e.g., Wilford et al., 2004), and Melton ratio (e.g.,
172 Bertrand et al., 2013) have demonstrated skill in discriminating the formative fan process. Not
173 surprisingly, these are the same catchment characteristics as those found here to be capable of
174 predicting debris-flow lobe-volume quantiles.

175 So why do these catchment characteristics determine process and lobe volume? Debris-flow
176 volume is a function of two elements: (1) the volume of the initiating failure or failures, and (2)
177 the volume changes, by entrainment and deposition, along the transport path (Jakob, 2005). In
178 the simplest case, debris flows may initiate on the steep slopes of the upper catchment, after
179 which they can grow in volume by eroding sediment while traversing through the catchment to
180 finally deposit on the fan. As such, for a given initial failure volume, the flow volume entering a
181 fan depends on the erosional potential of the debris flow and the amount of material available for

182 entrainment (e.g., Jakob et al., 2005). The entrainment rate at the base of a debris flow likely
183 increases with bed slope (e.g., Iverson & Ouyang, 2015), and therefore flow volume is likely to
184 increase with catchment relief (Fig. 3). Similarly, the larger the distance a debris flow traverses
185 through steep channels in a catchment, the larger the potential for net entrainment (assuming that
186 sufficient bed sediment exists and that its density and saturation are sufficient to promote
187 entrainment; Iverson, 2012), and the larger the flow volume may become. This may explain the
188 increasing flow-volume quantiles with catchment area, perimeter and length (Fig. 3). One should
189 note, however, that these effects are partly damped because the average catchment gradient
190 decreases with catchment area. Similarly, catchment length, perimeter and relief are strongly
191 related and increase logarithmically with basin area and the square-root of catchment area scales
192 linearly with basin relief, which defines the Melton ratio ($R^2 > 0.9$; Suppl. Fig. 4).

193 It is important to remember that our estimated volumes are based on the cross-sectional areas
194 of individual lobes, and will therefore underestimate the volume of large flows that form
195 multiple depositional lobes (e.g., Beaty, 1963; Blair and McPherson, 1998; 2009). Volume
196 estimates for flows forming multiple lobes, however, are only possible by direct measurement or
197 for the most recent events on a fan surface which have not been buried by subsequent flows. As
198 such, it is currently not possible to obtain large datasets of debris-flow volumes corrected for
199 multiple lobe formation. It is important to realize, however, that for some hazard applications
200 (such as damage to infrastructure) it is volume of sediment deposited at a point, rather than the
201 total flow volume that is most relevant. Our approach describes the probability to find a lobe of a
202 given size on a debris-flow fan, but for hazard assessment and mitigation it is also important to
203 understand the frequency of such flows. To advance the novel catchment-morphometry based
204 method to estimate debris-flow quantiles presented here, future research should thus focus on

205 direct estimation of flow volume-frequency distributions from a number of debris-flow
206 catchments in diverse climatic and lithological settings.

207

208 **CONCLUSIONS**

209 We have reconstructed debris-flow lobe-volume distributions from a large number of well-
210 preserved flow deposits on 10 fans in Saline Valley, California, USA, and compared lobe-
211 volume quantiles to a set of morphometric catchment characteristics. Our results show that, when
212 controlled for climatic and tectonic setting, lobe-volume quantiles, including 25, 50, and 75
213 percentiles and the maximum, depend on catchment area, length, perimeter, relief, and Melton
214 ratio. This implies that simple catchment characteristics, which can be extracted from globally-
215 available elevation datasets, may be used to obtain rough estimates of minimum flow design
216 volumes for sediment budgets as well as for hazard assessment and mitigation. While these
217 relationships are promising, future research should focus on the generation of flow volume-
218 frequency distributions from different climatic and lithological settings worldwide against which
219 to test the wider application of these estimates.

220

221 **ACKNOWLEDGMENTS**

222 Matthias Jakob and two anonymous reviewers helped to refine this paper. This work is funded by
223 the Netherlands Organization for Scientific Research (NWO) via Rubicon grant 019.153LW.002
224 to TdH. ALD acknowledges funding from the Institute of International Education via the Global
225 Innovation Initiative program.

226

227 **REFERENCES CITED**

228 Beaty, C. B., 1963, Origin of alluvial fans, White Mountains, California and Nevada, Ann.
229 Assoc. Am. Geogr., v. 53, p. 516–535.

230 Bennett, G. L., Molnar, P., McArdell, B. W., and Burlando, P., 2014, A probabilistic sediment
231 cascade model of sediment transfer in the Illgraben. *Water Resources Research*, v. 50, n. 2,
232 pp. 1225-1244.

233 Berti, M., and Simoni, A., 2007, Prediction of debris flow inundation areas using empirical
234 mobility relationships: *Geomorphology*, v. 90, no. 1, p. 144–161.

235 Bertrand, M., Liébault, F., and Piégay, H., 2013, Debris-flow susceptibility of upland
236 catchments, *Natural Hazards*, v. 67, p. 497-511.

237 Blair, T. C., and J. G. McPherson, 1998, Recent debris-flow processes and resultant form and
238 facies of the Dolomite alluvial fan, Owens Valley, California, *Journal of Sedimentary*
239 *Research*, v. 68, p. 800–818.

240 Blair, T. C., & McPherson, J. G., 2009, Processes and forms of alluvial fans. In *Geomorphology*
241 *of Desert Environments* (pp. 413-467). Springer, Dordrecht.

242 Bovis, M. J., and Jakob, M., 1999, The role of debris supply conditions in predicting debris flow
243 activity: *Earth Surface Processes and Landforms*, v. 24, p. 1039–1054.

244 Conrad, J. E., and McKee, E. H., 1985, Geologic map of the Inyo Mountains Wilderness Study
245 Area, Inyo County, California, Tech. Rep., USGS.

246 De Haas, T., Ventra, D., Carbonneau, P. E., and Kleinhans, M. G., 2014, Debris-flow dominance
247 of alluvial fans masked by runoff reworking and weathering. *Geomorphology*, v. 217, p.
248 165–181.

249 De Haas, T., Hauber, E., Conway, S. J., Van Steijn, H., Johnsson, A., and Kleinhans, M. G.,
250 2015, Earth-like aqueous debris-flow activity on Mars at high orbital obliquity in the last
251 million years. *Nature Communications*, v. 6(7543).

252 De Haas, T., van den Berg, W., Braat, L., and Kleinhans, M. G., 2016, Autogenic avulsion,
253 channelization and backfilling dynamics of debris-flow fans. *Sedimentology*, v. 63, no 6, p.
254 1596-1619.

255 De Haas, T., Densmore, A. L., Stoffel, M., Suwa, H., Imaizumi, F., Ballesteros-Cánovas, J. A.,
256 and Wasklewicz, T., 2018, Avulsions and the spatio-temporal evolution of debris-flow fans.
257 *Earth-Science Reviews*, v. 177, p. 53-75.

258 De Scally, F. A., & Owens, I. F. (2004). Morphometric controls and geomorphic responses on
259 fans in the Southern Alps, New Zealand. *Earth Surface Processes and Landforms*, v. 29, no.
260 3, p. 311-322.

261 Dowling, C. A., and Santi, P. M., 2014, Debris flows and their toll on human life: a global
262 analysis of debris-flow fatalities from 1950 to 2011. *Natural Hazards*, v. 71, no. 1, p. 203–
263 227.

264 Griswold, J. P., and Iverson, R. M., 2008, Mobility statistics and automated hazard mapping for
265 debris flows and rock avalanches. US Geological Survey Open-File Report 2007-5276.

266 Hungr, O., Morgan, G. C., and Kellerhals, R., 1984, Quantitative analysis of debris torrent
267 hazards for design of remedial measures. *Canadian Geotechnical Journal*, v. 21, p. 663–677.

268 Iverson, R. M., 2012, Elementary theory of bed-sediment entrainment by debris flows and
269 avalanches. *Journal of Geophysical Research: Earth Surface*, v. 117, F03006.

270 Iverson, R. M., Schilling, S. P., and Vallance, J. W., 1998, Objective delineation of lahar-
271 inundation hazard zones. *Geological Society of America Bulletin*, v. 110, no. 8, p. 972–984.

272 Iverson, R. M., and Ouyang, C., 2015, Entrainment of bed material by Earth-surface mass flows:
273 Review and reformulation of depth-integrated theory. *Reviews of geophysics*, v. 53, n. 1, p.
274 27-58.

275 Jakob, M., and Bovis, M. J., 1996, Morphometric and geotechnical controls of debris-flow
276 activity, southern Coast Mountains, British Columbia, Canada. *Zeitschrift für*
277 *Geomorphologie, Suppl.*, v. 104, p. 13–26.

278 Jakob, M., Bovis, M., and Oden, M., 2005, The significance of channel recharge rates for
279 estimating debris-flow magnitude and frequency. *Earth Surface Processes and Landforms*, v.
280 30, no. 6, p. 755–766.

281 Jakob, M., and Friele, P., 2010, Frequency and magnitude of debris flows on Cheekye River,
282 British Columbia. *Geomorphology*, v. 114, n. 3, pp. 382-395.

283 Jakob, M., Bale, S., McDougall, S., and Friele, P., 2016, Regional debris-flow and debris-flood
284 frequency-magnitude curves. *GeoVancouver 2016*.

285 Ma, C., Hu, K., and Tian, M., 2013, Comparison of debris-flow volume and activity under
286 different formation conditions. *Natural Hazards*, v. 67, n. 2, p. 261–273.

287 Marchi, L., and D'Agostino, V., 2004, Estimation of debris-flow magnitude in the Eastern Italian
288 Alps. *Earth Surface Processes and Landforms*, v. 29, n. 2, p. 207–220.

289 Oswald, J. A., and Wesnousky, S. G., 2002, Neotectonics and Quaternary geology of the Hunter
290 Mountain fault zone and Saline Valley region, southeastern California. *Geomorphology*, v.
291 42, n. 3, p. 255–278.

292 PRISM Climate Group, Oregon State University, 2015,
293 <http://www.prism.oregonstate.edu/normals/>.

- 294 Rickenmann, D., 1999, Empirical relationships for debris flows. *Natural hazards*, v. 19, n. 1, p.
295 47-77.
- 296 Schürch, P., Densmore, A. L., Rosser, N. J., & McArdell, B. W., 2011, Dynamic controls on
297 erosion and deposition on debris-flow fans. *Geology*, v. 39, p. 827-830.

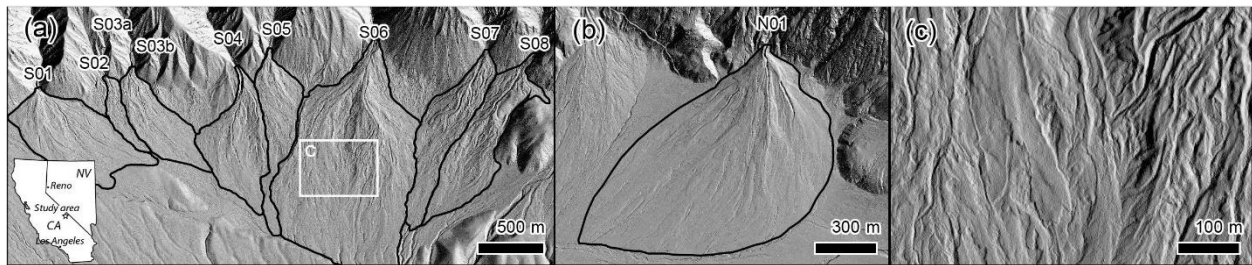
298 **TABLES.**

299 Table 1: Morphometric catchment characteristics.

Catchment	Dimensions	Symbol and definition
Area	m ²	A_c
Relief	m	H_c
Length	m	L_c
Perimeter	m	P_c
Mean slope	degrees	S_c
Melton ratio	-	$M_r = H_c/\sqrt{A_c}$
Relief ratio	-	$R_r = H_c/L_c$
Form factor	-	$F_f = A_c/L_c^2$
Elongation ratio	-	$E_r = (4A_c/\pi)/L_c$
Circularity index	-	$C_r = 4\pi A_c/P_c$

300

301 **FIGURE CAPTIONS**



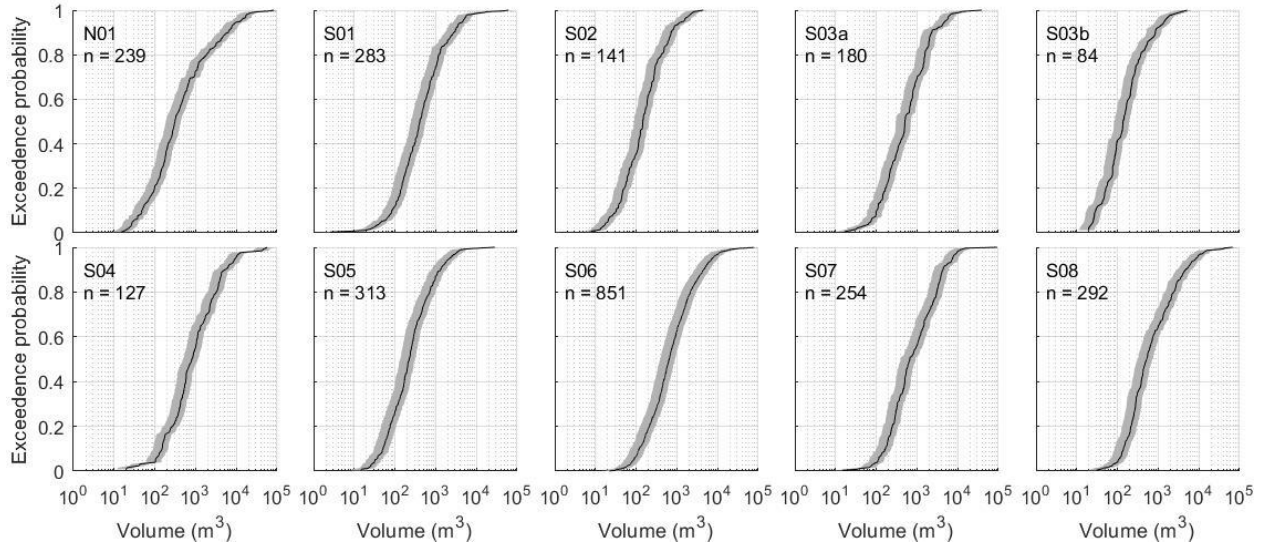
302

303 Figure 1. Debris-flow fans studied here. (a) Fans S01-08, on the southern margin of Saline

304 Valley. Fan apex of S05 is located at 6°34'28.85"N, 117°38'20.06"W. (b) Fan N01, on the

305 northern margin of Saline Valley. Fan apex is located at 36°49'31.66"N, 117°55'21.73"W. (c)

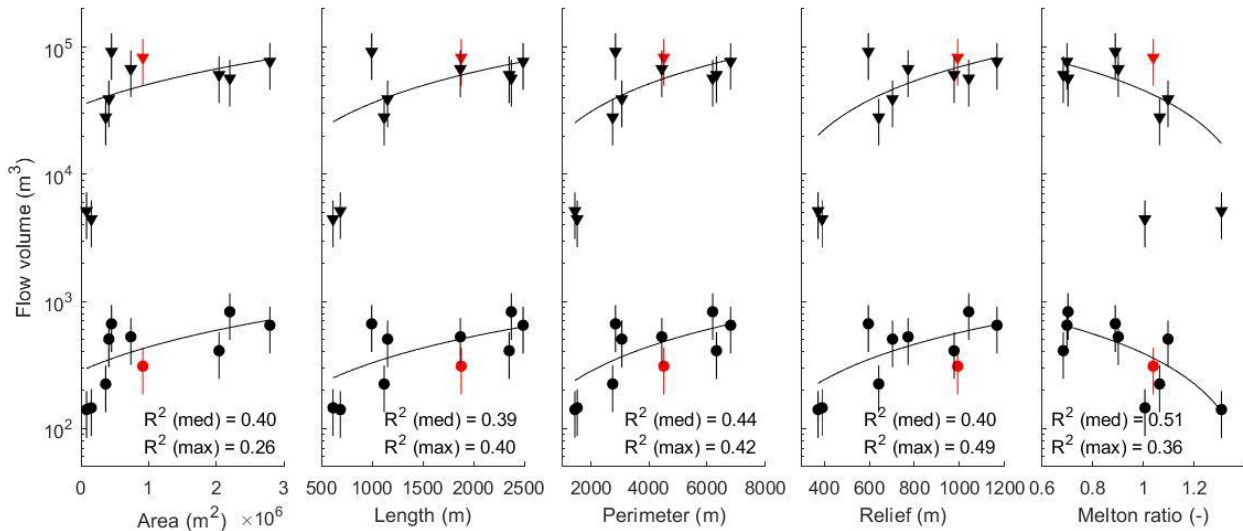
306 Detail of well-preserved debris-flow deposits on the surface of fan S06.



307

308 Figure 2. Cumulative lobe volume-frequency distributions for each fan. The gray bands indicate

309 the volume error range.



310

311 Figure 3. Catchment area, length, perimeter, relief, and Melton ratio plotted against median

312 (circles) and maximum (triangles) debris-flow lobe volumes. Vertical lines indicate the volume

313 error range. Black symbols are from quartz monzonite catchments S01-S08, while red symbols

314 are from catchment N01 underlain by metasedimentary rock. Linear regression lines are shown

315 for median and maximum lobe volumes.